but would give a smaller slope than the low molecular weight sample ($M = 6.5 \times 10^4$), which has undoubtedly been studied in its dilute concentration range.

Although the Varian Model 219 spectrophotometer that Destor et al.[8] used is roughly equivalent in its capabilities to the Perkin-Elmer Model 575 instrument, direct comparison of data would be difficult since the instruments operate on different principles. The Varian instrument is designed to automatically adjust slits to compensate for loss of intensity, which sacrifices spectral resolution. It can operate at a set resolution (fixed slits), but then sacrifices sensitivity. Both Perkin-Elmer instruments make scans at a fixed slit width to preserve resolution; and they compensate, in part, for the lower sensitivity by increasing the gain of the photomultiplier. Nonetheless, given the internal evidence afforded by our results with different cells and spectrophotometers, we propose that the apparent crossover seen by Destor et al.[8] is, like that we have obtained, an instrumental artifact despite its plausible molecular weight dependence. The lack of any real crossover in the concentration range where it should appear on the basis of simple physical reasoning, and where it has been detected in other properties, leads to the conclusion that ultraviolet absorption is not a useful method for detecting the onset of semidilute behavior in the systems considered here. For the reasons stated in the Introduction, we suspect that this insensitivity is a general one.

Acknowledgment. This work was supported by the Center for the Joining of Materials, Carnegie-Mellon University, through the National Science Foundation, Materials Research Section (Grant No. DMR76-81561).

References and Notes

(1) See, for example: Signer, R.; Cross, R. *Helv. Chim. Acta* **1934**, *17*, 59. Svedberg, T.; Pederson, K. O. "The Ultracentrifuge"; Oxford University Press: London, 1940; p 441. Campbell, H.; Johnson, P. *Trans. Faraday Soc.* **1944**, *40*, 221. Signer, R.; Egli, H. *Recl. Trav. Chim. Pays-Bas* **1950**, *69*, 45. Krigbaum, W. R.; Geymer, D. O. *J. Am. Chem. Soc.* **1959**, *81*, 1859. Benoit, H.; Picot, C. *Pure Appl. Chem.* **1966**, *12*, 545. Edwards, S. F. *Proc. Phys. Soc. London* **1966**, *88*, 265. Berry, G. C.; Fox, T. G. *Adv. Polym. Sci.* **1968**, *5*, 261. Mijnlieff, P.; Jaspers, W. *Trans. Faraday Soc.* **1971**, *67*, 1837.
(2) Flory, P. J. "Principles of Polymer Chemistry"; Cornell University Press: Ithaca, N.Y., 1953; Chapter 12.
(3) de Gennes, P. G. "Scaling Concepts in Polymer Physics"; Cornell University Press: Ithaca, N.Y., 1979. See also references therein.
(4) Cotton, J. P.; Farnoux, B.; Jannink, G.; Strazielle, C. *J. Polym. Sci., Polym. Symp.* **1973**, *No. 42*, 981.
(5) Cotton, J. P.; Farnoux, B.; Jannink, G. *J. Chem. Phys.* **1972**, *57*, 290. Daoud, M.; Cotton, J. P.; Farnoux, B.; Jannink, G.; Sarma, G.; Benoit, H.; Duplessix, R.; Picot, C.; de Gennes, P. G. *Macromolecules* **1975**, *8*, 804.
(6) Berry, G. C.; Nakayasu, H.; Fox, T. G. *J. Polym. Sci., Polym. Phys. Ed.* **1979**, *17*, 1825.
(7) Nyström, B.; Porsch, B.; Sundelöf, L.-O. *Eur. Polym. J.* **1977**, *13*, 683. Nyström, B.; Roots, J.; Bergman, R. *Polymer* **1979**, *20*, 157. Roots, J.; Nyström, B.; Sundelöf, L.-O.; Porsch, B. *Ibid.* **1979**, *20*, 337. Destor, C.; Rondelez, F. *J. Polym. Sci., Polym. Lett. Ed.* **1979**, *17*, 527. Pouyet, G.; Dayantis, J. *Macromolecules* **1979**, *12*, 293. Roots, J.; Nyström, B.; Roots, J. *J. Macromol. Sci., Rev. Macromol. Chem.*, in press.
(8) Destor, C.; Langevin, D.; Rondelez, F. *J. Polym. Sci., Polym. Lett. Ed.* **1978**, *16*, 229.
(9) Berry, G. C.; Hobbs, L. M.; Long, V. C. *Polymer* **1964**, *5*, 31.
(10) Kalpagam, V.; Rao, R. *J. Polym. Sci., Part A* **1963**, *1*, 233.
(11) Effective exclusion of oxygen would require purging the entire optical system, as well as the sample compartment and the solution, with nitrogen. Only measurements below 200 nm might be affected by oxygen; however, since our POE samples (unlike most of those of Destor et al.[8]) contained no carbazole end groups, our ability to analyze data at wavelengths above 200 nm would not be impaired.
(12) The POE absorbances at 210 nm show considerable scatter since they were obtained directly from plots of spectra recorded with λ_{max} adjusted to full scale (see Figure 1).
(13) This experiment may not be strictly comparable with corresponding measurements on the other PVAc samples since it was made later, after a routine instrument servicing.

Raman Spectroscopic Study of the High-Pressure Phase of Polyethylene

Stephanie L. Wunder*

Optical Sciences Division, Naval Research Laboratory, Washington, D.C. 20375.
Received February 3, 1981

ABSTRACT: The Raman spectra of polyethylene at 5.1 kbar were obtained as a function of increasing temperature in the orthorhombic, intermediate, and melt phases. It was found that a plot of $r = I(1130)/I(1090)$, an order parameter related to the relative concentration of trans bonds, vs. temperature, T, was sigmoidal. The steepest change of r with T occurred in the intermediate phase. Comparison of r values in the intermediate phase with an approximate calibration curve and with values obtained from lipid membrane phase transition data indicates that the intermediate phase has significant but variable trans bond population, ranging from 62 to 68%. Analysis of the high-frequency C–H stretching region, which is indicative of changes in lateral order as well as changes in chain conformation, indicates that the intermediate phase has hexagonal symmetry, in agreement with X-ray data, and also reflects the changing trans bond ratio in this phase. Preliminary evidence on chain conformation in the melt as a function of increasing pressure points to preferential gauche bond formation at high pressures.

Introduction

The high-pressure phase of polyethylene (PE), discovered by Bassett and Turner[1] and Yasuniwa and Takemura,[2] occurs below its melting temperature at pressures above ~3 kbar. While the ordinary crystal structure of PE is orthorhombic, the structure of the intermediate phase was determined to be hexagonal by Piermarini et al.[3] The properties of this intermediate phase are important because the resultant crystalline morphology of PE is dependent upon whether or not this phase is traversed upon crystallization, either by cooling or by pressurization. When PE is crystallized below ~3 kbar, its morphology is lamellar. However, above this pressure, when the intermediate phase interposes between the crystal and the melt, the morphology commonly known as

* Address correspondence to author at Polymer Science and Standards Division, National Bureau of Standards, Washington, D.C. 20234.

the "extended-chain crystal" (ECC) results.

As discussed in Leute and Dollhopf's review[4] of the experimental data in the literature on the high-pressure phase of PE, most of the available information about the phase comes from calorimetry and X-ray scattering. Experimental evidence about the detailed molecular structure of the phase is scarce and comes mostly from the work of Takemura et al.[5,6] Using ultrasonic measurements and Raman and NMR studies at high pressure, they demonstrated that the physical properties of the phase were more similar to those of the melt than to those of the solid. Analysis of X-ray data also indicated the presence of conformational disorder.[7,8] This evidence of disorder coupled with the known hexagonal packing suggested a liquid crystallike structure for the phase; this hypothesis was supported by optical microscopic observation.[9] Recently, Takemura et al.[6] used Raman spectroscopy as a direct measure of chain conformation in the intermediate phase. In the present paper we used the same technique to study the conformational changes which occur in the intermediate phase as a function of temperature at 5.1 kbar. Four regions of the spectra are analyzed: the skeletal optical modes (SO) between 950 and 1200 cm^{-1}, the C–H twisting vibration at 1300 cm^{-1}, the C–H bending region between 1400 and 1500 cm^{-1}, and the C–H stretching region between 2750 and 3050 cm^{-1}. The skeletal optical modes are used as a relative measure of trans bond population. It is found that a plot of $r = I(1130)/I(1090)$, an order parameter related to the concentration of trans bond, vs. temperature, T, is sigmoidal. The steepest change of r with T occurs in the intermediate phase, which spans at most a 10 °C temperature interval. Comparison of r values with those obtained from lipid membrane phase transition data in the literature indicates that the intermediate phase has a significant but variable trans bond population. The bands in the C–H bending and stretching regions are used as measures of both molecular conformation and intermolecular order. Our results differ with those of Takemura et al.[6] in the latter two spectral regions. Our C–H bending and stretching regions are consistent with the known features of the orthorhombic, hexagonal, and melt spectra of alkanes and PE at ambient pressures. The combined evidence that the high-pressure phase is conformationally disordered, as is the liquid, but also has a hexagonal structure points to its liquid-crystallike nature. We are thus in agreement with the conclusion of Takemura et al.[6] on this point. The evidence of variable conformational structure in the intermediate phase is a new piece of experimental data which may help to explain the thermodynamic stability of this phase with respect to that of the orthorhombic crystal.

Experimental Section

The Raman spectra of PE were obtained in a hydraulic high-pressure vessel designed by Daniels. In this system, the polyethylene is contained in a $^1/_4$-in. length of Tygon Fluron tubing of $^1/_8$-in. inner diameter and $^1/_{16}$-in. wall thickness between two 0° material sapphire windows of $^3/_{32}$-in. diameter and $^3/_{16}$-in. width. A PE pellet is inserted in the tube with the sapphire windows loosely in place at either end. This assembly is heated to 145 °C; when the PE melts, the two sapphires are pressed toward each other to mold a PE plug which makes a smooth interface with the windows and excludes air. One of the windows forms a pressure seal in the pressure vessel and is used for optical access. The high-pressure cell, whose dimensions were approximately 2 in. (D) × $1^3/_8$ in. (L), was mounted in a Fisher Model 177 forced convection oven, modified with evacuated windows for optical access. Pressure was measured with an American Instrument Co. 100 000-psi pressure gauge, accurate to ±0.1 kbar. Two copper–constantan thermocouples were placed on the body of the cell and in the air in the immediate vicinity of the cell. The cell in the thermostated chamber was equilibrated until the temperature readings on the thermocouples were within 1 °C of each other. The Raman spectra of PE at ambient pressure as a function of temperature were obtained with the sample in a quartz capillary mounted in a temperature-controlled heating iron; temperatures were maintained to ±0.5 °C in this arrangement.

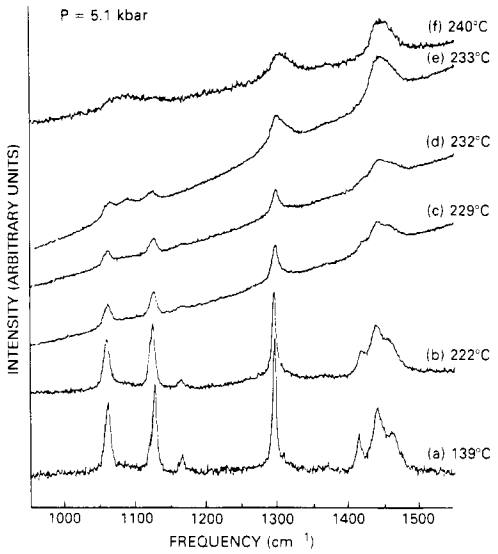

Figure 1. Raman spectra of PE at 5.1 kbar in the region 950–1550 cm^{-1} at (a) 139, (b) 222, (c) 229, (d) 232, (e) 233, and (f) 240 °C.

Raman spectra were obtained in the backscattering geometry. The experimental setup is described elsewhere.[10] The exciting source was either 514.5-nm light from a Coherent Radiation Model 52 argon ion laser or 647.1-nm light from a Coherent Radiation Model 750K krypton laser. Between 200 and 400 mW of incident radiation was used. A Spex 14018 double monochromator with holographic gratings, Spex DPC2 photon-counting equipment, and an RCA C31034A photomultiplier tube were used to collect the Raman scattered light. Since no difference was observed in the spectra taken with 200- and 600-μm slit widths (3- and 9-cm^{-1} band-pass, respectively), the larger slits were used to obtain better signal-to-noise ratios. At high temperatures in particular it was necessary to obtain the spectra as quickly as possible because sample deterioration and the concomitant fluorescence were a serious problem in data acquisition. Green light seemed to accelerate this process, so the red laser line was used at the highest temperatures.

The polyethylene sample used for this study was linear polyethylene SRM 1475 (52 000 weight-average molecular weight), obtained from the National Bureau of Standards. The characteristics of this material can be found in NBS special publication 260-42. It was used because the high-pressure X-ray experiments of Yamamoto et al.[8] had utilized the same material, so its phase diagram was well established.

Results

Raman spectra of PE at 5.1 ± 0.1 kbar between 138 and 240 °C are shown in Figure 1, which spans the frequency interval 950–1550 cm^{-1}, and in Figure 2, which spans the region 2750–3050 cm^{-1}. The spectra are representative of two phases of PE, an orthorhombic solid phase and a hexagonal intermediate phase; other spectra at intermediate temperatures were also obtained and used in subsequent data analysis but are not shown. The difference in the high-frequency spectra between the hexagonal phase and the melt is shown in Figure 3 for the case of PE at 225 °C at 2.7 and 4.1 kbar; at 2.7 kbar PE is molten while at 4.1 kbar it is in the intermediate hexagonal phase. Because of the fluorescence problem at high temperatures, it was difficult to obtain spectra of good signal-to-noise ratio in the melt spectrum of PE at 5 kbar above 260 °C. Figure 4 is the melt spectrum of PE at atmospheric pressure as a function of increasing temperature in the region 950–1550

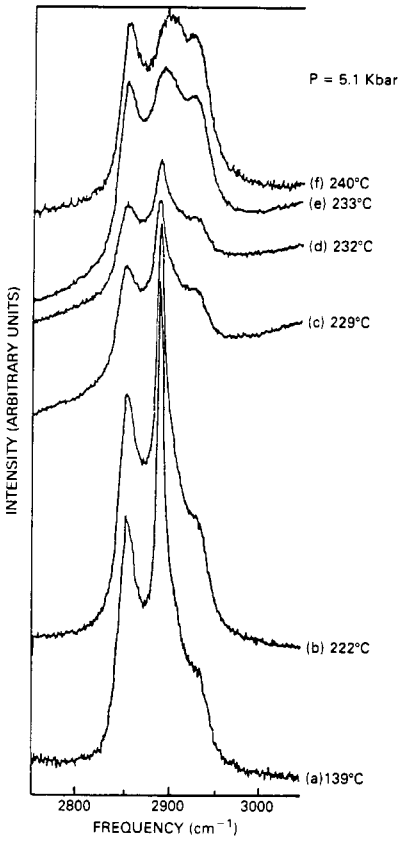

Figure 2. Raman spectra of PE at 5.1 kbar in the region 2750–3050 cm^{-1} at (a) 139, (b) 222, (c) 229, (d) 232, (e) 233, and (f) 240 °C.

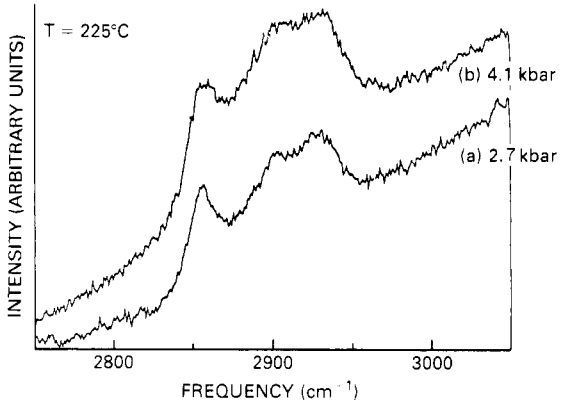

Figure 3. Raman spectra of PE at 225 °C in the region 2750–3050 cm^{-1} at (a) 2.7 kbar (melt) and (b) 4.1 kbar (intermediate phase).

cm^{-1}; Figure 5 spans the region 2750–3050 cm^{-1}.

Discussion

Raman spectroscopic data on PE at high temperatures and pressures are a rich although complex source of information on the molecular conformations and intermolecular interactions of the chains. In the following discussion the data will be analyzed in the regions 950–1550 and 2750–3050 cm^{-1} in light of what is known both experimentally and theoretically about the molecular vibrations in these regions at atmospheric pressure. The analysis is facilitated by the large body of Raman experiments on phase transition data of lipid membrane in the literature (e.g., ref 11–17) and by the recent theoretical advances of Zerbi et al.[18] and Synder et al.[19,20] in elucidating the origin of the band shapes in the high-frequency C–H stretching region.

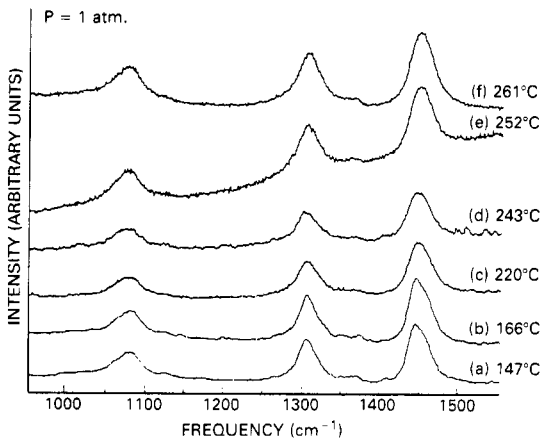

Figure 4. Raman spectra of PE in the melt at atmospheric pressure in the region 950–1550 cm^{-1} at (a) 147, (b) 166, (c) 220, (d) 243, (e) 252, and (f) 261 °C.

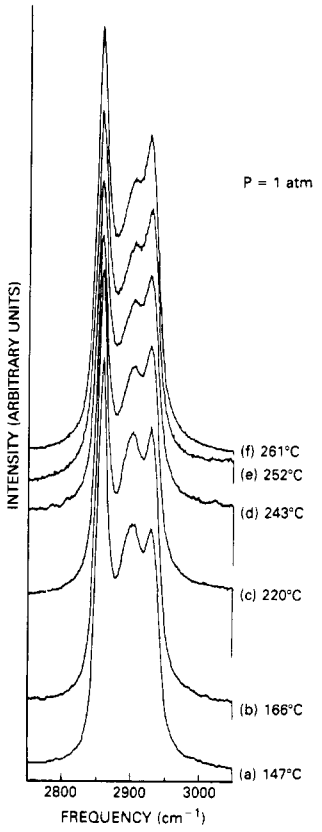

Figure 5. Raman spectra of PE in the melt at atmospheric pressure in the region 2750–3050 cm^{-1} at (a) 147, (b) 166, (c) 220, (d) 243, (e) 252, and (f) 261 °C.

Although ideally one would like to obtain Raman measurements for regions of the phase diagram determined by another means (i.e., calorimetrically or via X-ray scattering), the accuracy of previous work in the literature is worse than that obtained in this study. The phase diagrams for PE in the literature[1,4,8,10] depend upon the sample used in the study, whether the phase diagram was obtained upon heating or cooling, and upon the experimental method employed to obtain the transition points. In addition, measurements obtained in the diamond anvil cell (DAC) are at variance with those obtained from other high-pressure experiments. This was shown to be due to severe radial and axial temperature gradients which can arise when the DAC is heated, decreasing the accuracy of the temperature and, thus, also the pressure determination.[21] In the present experiment, pressures are accurate

to ±0.1 kbar and temperatures to ±0.5 °C. No calorimetric or X-ray data achieve this accuracy for the PE sample studied; the phase transition points from orthorhombic crystal to hexagonal intermediate to melt are therefore determined on the basis of their Raman spectra, as discussed in more detail below. Just as the 110 and 100 Bragg reflections of X-ray scattering are used to identify the hexagonal crystal and the 011, 111, 110, and 200 reflections to identify the orthorhombic lattice, Raman spectroscopic features of these phases can be used to identify them.[19] In particular, characteristic crystal field splittings of the orthorhombic lattice in the C–H bending and stretching regions will be used to detect the occurrence of this phase. The hexagonal lattice can similarly be identified by its characteristic high-frequency region. Parts a and b of Figure 1 for PE at 5.1 kbar and 139 and 222 °C, respectively, are the characteristic spectra for an orthorhombic crystal in the C–H bending region; parts a and b of Figure 2 are the characteristic spectra in the C–H stretching region. Parts e and f of Figure 2 of PE at 5.1 kbar and 233 and 240 °C, respectively, are typical Raman spectra for a hexagonal lattice. The spectra in Figures 1c,d and 2c,d are believed to be mixed-phase spectra—that is, a coexistence region of hexagonal intermediate and folded-chain orthorhombic crystal (fcc). Evidence for this mixed-phase region comes also from the X-ray scattering data of Takemura et al.;[6,7] 100 hexagonal and 110 and 200 orthorhombic reflections were observed simultaneously. From the Raman spectroscopic data of PE at 5.1 kbar as a function of temperature, the transitions observed are as follows: 229 °C, orthorhombic solid → mixed fcc orthorhombic–hexagonal intermediate phase; 233 °C, mixed phase → hexagonal intermediate phase; 241 °C, hexagonal intermediate → melt.

The subsequent discussion is a more detailed analysis of the spectra divided into the four spectral regions studied, the skeletal optical modes and the CH_2 twisting, bending, and stretching vibrations.

Skeletal Optical Modes. The bands in the region 950–1250 cm^{-1} are the skeletal optical modes; they belong to the ν_4 branch of the dispersion curve of PE whose normal coordinates are a combination of C–C stretching and bending motions.[22] In alkane crystals, where the chain is in the all-trans conformation two bands at 1064 and 1130 cm^{-1} appear in the Raman spectrum. Upon melting of the crystals, these bands are greatly diminished in intensity and a broad envelope of bands centered around 1090 cm^{-1} appears whose intensity results from conformers with gauche bonds. In the case of PE, where there is always residual amorphous material, the Raman spectrum of the solid has a very weak band at 1090 cm^{-1} in addition to the two all-trans bands at 1064 and 1130 cm^{-1}. The ratio, R, of the intensity of either the 1064- or the 1130-cm^{-1} band, $I(1064)$ or $I(1130)$, to the intensity of the 1090-cm^{-1} band, $I(1090)$, can be viewed as a microscopic order parameter related to the statistical populations of translationally ordered trans bond sequences.[11] r was observed to increase by Strobl and Hagedorn[23] for branched PE as a function of temperature in the solid state (from −40 to +80 °C), reflecting partial melting of the branched sample. In lipid membrane systems, whose alkane tails have a high but variable degree of longitudinal order, changes in R have been used extensively to follow the gel–liquid crystal phase transition in these systems;[11–17] the midpoint of the sigmoidal plot of r vs. T yields a transition temperature in good agreement with that obtained calorimetrically. The spectra in Figures 1 and 4 at elevated pressure can be understood in light of what is known about these similar

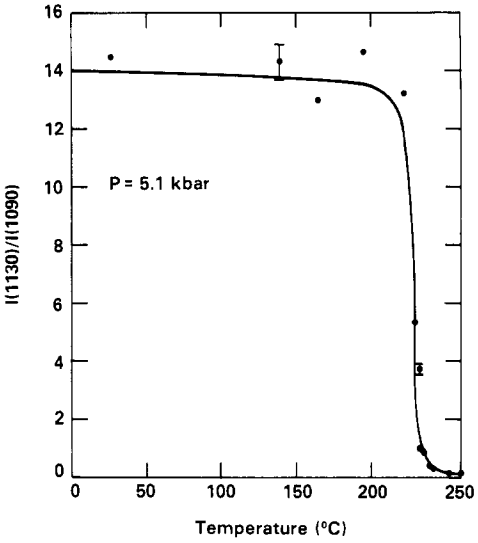

Figure 6. Plot of $r = I(1130)/I(1090)$ vs. temperature for PE at 5.1 kbar.

systems at ambient pressure. At 5.1 kbar, between 139 and 232 °C, the spectra in the skeletal optical region are similar to that observed for PE at ambient conditions; most of the intensity appears in the 1064- and 1130-cm^{-1} bands, with a small contribution arising from gauche conformers at 1090 cm^{-1}. By comparison, the melt spectrum of PE at atmospheric pressure between 147 and 261 °C shown in Figure 4 has most of the SO intensity in the 1090-cm^{-1} envelope. At 147 and 166 °C in the melt weak but discrete bands at 1064 and 1130 cm^{-1} due to residual trans bands can still be observed; at higher temperatures the 1130-cm^{-1} band is observed very weakly, but the 1060-cm^{-1} band merges with the 1090-cm^{-1} band.

In Figure 1e,f it can be seen that in the spectra at 233 and 240 °C, the 1064-, 1090-, and 1130-cm^{-1} peaks appear at of roughly equal intensity. Three other spectra, at 235, 236, and 239 °C (not shown), have band intensities intermediate between those of Figure 1e and Figure 1f. These spectra are similar to ones observed in biomembrane systems. A plot of r vs. T for PE at 5.1 kbar is shown in Figure 6. The plot is sigmoidal, as is observed in biomembrane phase transition data. The error bars in Figure 6 are greatest at low and high trans content, since at these extremes either the 1130- or 1090-cm^{-1} band approaches zero. The steepest change of r with T occurs in the intermediate phase. The trans bond population in this phase can be estimated as follows.

A calibration curve for $r = I(1130)/I(1064)$ vs. gauche bond population was obtained under the assumption that in amorphous PE the relative bond populations obey Boltzmann statistics with pentane exclusion. The isomerization energy between trans and gauche bonds was taken as 600 cal/mol. For PE crystallized in the ECC, the value of R approaches infinity as the number of gauche bonds approaches zero. Above 140 °C, in the melt spectrum of PE (Figure 3), r becomes small as the number of trans bonds diminishes. Even in the melt, however, it should be noted that the trans bond population is high (about 60%). For points between these two extremes, the data in Figure 1 for PE of about 75% crystallinity and the data of Stobl and Hagedorn[23] for a branched PE sample of relatively low percent crystallinity were analyzed. The r values of the spectra of the latter material in the SO region at −40, 25, and 80 °C were measured from Figure 3 of ref 23. The percent crystallinity for these same samples was obtained from Figure 4 of the same reference. It was assumed that the noncrystalline material obeyed

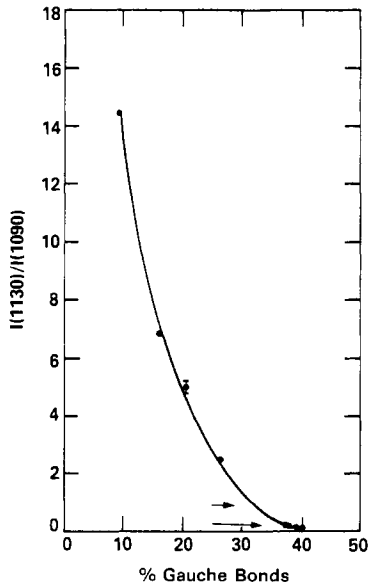

Figure 7. Calibration curve of $r = I(1130)/I(1090)$ vs. gauche bond population for PE. The smooth curve is included as a guide for the eye. Arrows bracket R values observed in the intermediate phase of PE.

Boltzmann statistics with pentane exclusion, and a number for the percent gauche bonds was then extracted. A similar calculation was done for PE SRM 1475. The results of these calculations are shown in Figure 7. It can be seen that the variations of r with trans-to-gauche ratio is very nonlinear. Nevertheless, since R values in the intermediate phase range between 1.0 and 0.3, the corresponding percent trans bonds in this phase estimated from the calibration curve lie between 62 and 68%. This figure is consistent with relative bond populations expected in the liquid-crystalline phase of biomembranes whose r values are similar.[24] It should be noted that the absolute nature of these results is limited by the inherent temperature dependence of the Raman scattering, which may not be the same for all the bands.

CH_2 Twisting Vibration. The CH_2 twisting vibration near 1300 cm^{-1} has been shown to be useable as an internal intensity standard by Strobl and Hagedorn;[23] they demonstrated that the integrated scattering intensity in this frequency range is independent of chain conformation. For extended-chain PE (>98% crystallinity), the CH_2 twisting vibration occurs at 1295 cm^{-1}. For melted PE a broad amorphous band with a maximum at 1303 cm^{-1} occurs, as can be seen in Figure 4. For the temperature interval studied in the melt, 148–260 °C (Figure 4a–f), the band broadens slightly, the full width at half maximum (fwhm) varying from 27 to 33 cm^{-1}. The peak position remains invariant, however. For PE which is partially crystalline, Strobl and Hagedorn[23] also demonstrated that the spectrum in the CH_2 twisting region could be represented by a superposition of the crystalline and amorphous bands. Thus in Figure 1a,b, for PE at 5.1 kbar and 139 and 222 °C, respectively, the small high-frequency tail on the 1300-cm^{-1} band arises from the amorphous component. It is less pronounced than that which occurs for the branched, partially crystalline PE sample studied by Strobl and Hagedorn, which contains more amorphous material. The fwhm of orthorhombic crystalline PE, at atmospheric pressure and at 5.1 kbar from 25 to 222 °C, is 5 cm^{-1}. By contrast, in the region believed to be a mixed phase, at 5.1 kbar and 229 and 232 °C (Figure 1c,d) the fwhm is 11 and 13 cm^{-1}, respectively. In the intermediate phase, at 5.1 kbar between 233 and 240 °C, the fwhm is 30 ± 3 cm^{-1}. The fwhm in the hexagonal phase is, thus, within experimental error, the same as that in the melt-phase spectra. The fwhm in the cases believed to be mixed-phase spectra fall between those of the crystal and the hexagonal phase. In addition, the peak position shifts from 1279 cm^{-1} in the crystal phase to 1302 cm^{-1} in the intermediate hexagonal phase.

CH_2 Bending Vibrations. The origin of the complex structure in the CH_2 bending region has been studied by Zerbi[18] et al. and Snyder et al.[19,20] For the orthorhombic crystal, there are three bands in the spectrum at room temperature and pressure: a fundamental at 1442 cm^{-1} (A_g) is crystal field split into two components at 1418 (A_g) and 1449 cm^{-1} (B_{3g}); the latter then interacts via Fermi resonance with overtones of the 720-cm^{-1} infrared active rocking fundamental, giving rise to bands at 1440 and 1462 cm^{-1}. These three bands can be observed in PE at room temperature and pressure and in PE at 5.1 kbar from 25 to 232 °C (Figure 1). The band at 1418 cm^{-1} is associated with the orthorhombic crystal structure. Unlike the Raman spectra observed by Takemura et al.[6] under similar conditions, the characteristic 1418-cm^{-1} band for the orthorhombic crystal is seen to persist until formation of the hexagonal phase. This is consistent with the X-ray data of Yamamoto et al.,[8] who observed no change in the X-ray diffraction pattern of PE under high pressure with increasing temperature until the phase transition to the hexagonal phase occurred.

In the room-pressure hexagonal rotator phase of n-alkanes, the 1418-cm^{-1} band disappears since the crystal lattice must have two molecules per unit cell for crystal field splitting to occur and the hexagonal crystal has only one molecule per unit cell. Although the CH_2 bending modes broaden with increasing T, the disappearance of structure in this region at 233 °C (Figure 1) is not due to temperature broadening, but rather to a morphological change. This is demonstrated by increasing P at 233 °C: the triplet structure reappears. Between 233 and 240 °C at 5.1 kbar (Figure 1) the CH_2 bending vibration is a broad singlet centered around 1440 cm^{-1}. Its full width at half maximum (fwhm) is about 38 cm^{-1}. The melt spectrum of PE in this region at atmospheric pressure shown in Figure 4 also has one band centered around 1440 cm^{-1} whose fwhm is about 32 cm^{-1}. The difference in the fwhm between the melt spectra and the intermediate-phase spectra (6 cm^{-1}) might be indicative of weak Fermi resonance structure in the latter.

The occurrence of the 1418-cm^{-1} band in Figure 1c,d together with the intermediate value of the fwhm of the CH_2 twisting band suggests that these figures are spectra of a mixed phase. However, an orthorhombic structure somewhat disordered by pretransition fluctuations cannot be ruled out.

CH_2 Stretching Region. The origin of the complex band structure in the CH_2 stretching region arises from three sources: (1) intramolecular Fermi resonance resulting from interaction of the symmetric C–H stretching fundamental, A_g, with binary combinations of methylene bending modes (i.e., chain conformation effects), (2) intermolecular Fermi resonance of these same modes perturbed by crystal interactions (i.e., chain packing effects), and (3) chain mobility.[18,19,20,24]

The melt spectrum of PE at atmospheric pressure as a function of temperature, Figure 5, displays three discrete bands: a strong narrow band at 2850 cm^{-1} and two broader bands at 2898 and 2930 cm^{-1}. The nature of the Fermi resonance, which determines the detailed structure in this region, depends on the density of phonon states in the

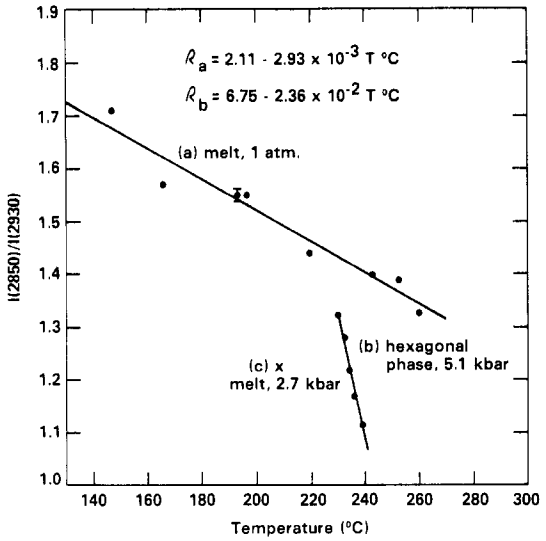

Figure 8. Plots of $R = I(2850)/I(2930)$ vs. temperature for PE at (a) atmospheric pressure (melt), (b) 5.1 kbar (intermediate phase), and (c) 2.7 kbar (melt (×)).

bending region. Disruption of the translationally invariant all-trans structure by the introduction of gauche bonds or other type of dihedral angle disorder modifies this density of states. According to Zerbi,[18] in the presence of an increased concentration of trans bonds the intensity of the band at 2930 cm^{-1}, $I(2930)$, is expected to decrease while the intensity of the peak at 2850 cm^{-1}, $I(2850)$, should increase. This trend is observed in the melt spectra of Figure 5a–f: as temperature is increased, changing the Boltzmann populations to favor gauche conformers, the 2930-cm^{-1} band is seen to increase relative to the 2850-cm^{-1} band. A plot of the ratio $R = I(2850)/I(2930)$ vs. temperature, Figure 8a, is linear; the data points can be fitted by a straight line given by

$$R = 2.11 - 2.93 \times 10^{-3}T\ °C \qquad (1)$$

with a confidence level of 97.4%.

The spectra of PE at 5.1 kbar from 25 to 222 °C display three bands: a narrow band at 2887 cm^{-1}, a slightly broader band at 2850 cm^{-1}, and a shoulder at 2930 cm^{-1}. The narrow band at 2887 cm^{-1} is the antisymmetric C–H stretching fundamental, B_{1g}. The band at 2850 cm^{-1}, the shoulder at 2930 cm^{-1}, and most of the intensity underlying the 2887-cm^{-1} band arise from a Fermi resonance interaction between a continuum of overtones of the CH_2 bending fundamental with the symmetric CH stretching vibration. The shapes of these broader secondary maxima depend on the dispersion of the bending mode fundamental, which, in the case of a crystal, is dependent on its structure. Parts a and b of Figure 2 are characteristic of the C–H stretching region for an orthorhombic crystal; the same spectrum is observed for PE at ambient conditions. As was the case for the CH_2 bending region, the characteristic orthorhombic Raman spectra persists until transition to the hexagonal phase occurs.

In Figure 2e,f, obtained in the intermediate phase, two changes in the spectra occur. The sharp 2887-cm^{-1} band decreases in peak height, broadens considerably (from about 6 to about 30 cm^{-1}), and shifts in frequency to 2900 cm^{-1}. In addition, the 2930-cm^{-1} shoulder becomes a well-defined peak. These spectral features reflect two changes occurring in the intermediate phase: a change in the packing arrangement to the hexagonal structure and an increase in disorder of the chains.

It is difficult to resolve into separate components the several contributions to the changing shape of the C–H stretching region. Nevertheless, one can draw upon previous work on biomembrane structure, whose Raman spectra are dominated by vibrations of the fatty acyl chains, to elucidate the causes of the changes taking place. It is known[11-17] that disruption of regular chain packing in lipid bilayers, either by melting or by dissolution, results in a decrease in the intensity of the 2887-cm^{-1} band relative to the 2850-cm^{-1} band, as is observed in Figure 2e,f compared to Figure 2a,b. In addition, from the theoretical work of Zerbi et al.[18] and the experiments of Wunder et al.,[26] it is known that the increases in the 2930-cm^{-1} band relative to the 2850-cm^{-1} band observed in these same figures are indicative of decreases in trans bond populations. In the intermediate phase, a plot of R vs. T is observed to be linear (Figure 8b), as was the case for molten PE. The points in Figure 8b can be fitted by a straight line given by

$$R = 6.75 - 2.36 \times 10^{-3}T\ °C \qquad (2)$$

with a 98.8% confidence level. The slope in the intermediate phase is about an order of magnitude larger than that in the melt, but the magnitude of R in the temperature region studied is lower. Unfortunately, since intensities in the high-frequency region are strongly affected by intermolecular interactions, it is not possible to extract numerical values of trans bond populations in the intermediate phase by comparison with R in the fluid. Nevertheless, the fairly large change of R with T in this small (~8 °C) temperature interval provides substantiating evidence for the changing trans bond population in the intermediate phase which was observed more directly in the skeletal optical region of the spectrum.

The upward frequency shift (of about 10 cm^{-1}) of the 2887-cm^{-1} band is also associated with destruction of the translationally ordered trans structures. This has been deduced by isotopic dilution studies of alkane chains in deuterated crystal matrices: the all-trans chain experiences no frequency shift of the asymmetric C–H stretching vibration upon dilution.[19]

The isotopic dilution studies of Snyder et al.[19] are also useful in elucidating the effects of interchain interactions (or "perpendicular dispersion") on the shape of the broad secondary maxima in the C–H stretching region. In particular, for the hexagonal structure compared with the isolated chain, the 2850-cm^{-1} band is asymmetric, and there is considerable filling in of the trough between the 2850-cm^{-1} band and the 2887-cm^{-1} band (cf. Figure 2a,b), as is also observed for the orthorhombic crystal. This effect is noticed, but not as dramatically, by a comparison between the hexagonal and melt phases, Figure 3b,a, respectively. There is, of course, no perpendicular dispersion in the melt phase.

A comparison of the high-frequency spectra of the intermediate phase with that of the rotator-phase spectra of alkanes (the solid-state hexagonal phase occurring a few degrees below their melting points; see, for example, Figure 2e, ref 19), suggests a similar hexagonal packing order. However, the rotator phase is a solid crystal phase with the chains in the all-trans configuration. Thus the intensity ratio of the 2930-cm^{-1} band with respect to the 2850-cm^{-1} band is small compared to the ratio in the high-pressure intermediate phase which contains disordered structures. In this connection, it should also be noted that in the SO region the rotator phase spectrum has intensity only in the 1064- and 1130-cm^{-1} trans bands,[27] with no intensity in the 1090-cm^{-1} gauche envelope; this is in contrast to the high-pressure intermediate-phase spectra in this region, where all three bands have sizeable intensity.

Thus the spectra in Figure 2e,f are consistent with a hexagonal packing arrangement with some longitudinal disorder resulting from the introduction of gauche bonds or from a more general type of disorder of the chain dihedral angles. As pointed out by a reviewer, it is not possible from the vibrational spectra alone to distinguish between a true hexagonal structure and an effective hexagonal structure since for both cases, factor-group splitting will not appear. The latter may involve long-range disorder along with some degree of local order. It should also be noted that Snyder et al.[25] recently associated the broadening of the 2887-cm^{-1} band with chain mobility, which was defined as the freedom of the extended chain to rotate and twist about its long axis. Since considerable broadening occurs in the 2887-cm^{-1} band in the intermediate phase, this mechanism might be a contributing factor.

Spectra 2c and 2d are believed to be mixed-phase spectra. The band profiles in the C–H stretching region are intermediate between those of the orthorhombic phase and the hexagonal phase. However, as noted above, the Raman data are also consistent with a pretransitionally disordered orthorhombic structure. A further study of hysteresis effects in this temperature and pressure range is being pursued.

One other interesting feature arises in the analysis of the high-frequency C–H stretching region. A comparison of the melt spectrum of PE at 220 °C and atmospheric pressure, Figure 5c, and that of PE at 225 °C and 2.7 kbar, Figure 3a, indicates a large change in R with pressure in the melt. The value of R for the spectrum in Figure 3a is indicated by a × in Figure 8c. According to Zerbi's analysis, a decrease in R, or an increase in the intensity of the 2930-cm^{-1} band with respect to that of the 2850-cm^{-1} band, is indicative of an increasing gauche band population. To attain the same value of R as is observed for the high-pressure melt of PE, the temperature of the atmospheric melt would need to be increased by 105 °C if the plot of R vs. T, Figure 8a, continued to be linear. If PE is assumed to be isotropic in the melt, obeying Boltzmann statistics with pentane exclusion, then the 105 °C shift corresponds to a gauche bond population about 2% higher than that at 225 °C and 1 atm. Experimental evidence for preferential gauche bond formation with increased pressure in the melt was observed for the lower molecular weight alkanes by Schoen et al.,[28] using low-frequency Raman bands sensitive to conformer populations and for butane by Lascombe et al.[29] The preliminary finding of this effect in PE will be pursued in a more systematic study of the effects of pressure on the high-frequency melt spectrum.

Conclusions

Raman spectroscopy has been used as a microscopic probe of chain conformation and environment. It was found that the high-pressure intermediate phase of polyethylene is characterized by a hexagonal structure with partial destruction of the longitudinal order resulting from disorder of the chain dihedral angles and/or introduction of gauche bonds in the chain. This is consistent with the hypothesis of a type of liquid crystalline state for this phase. The degree of disorder was found to be a function of temperature in the intermediate phase. Preliminary evidence of chain conformation in the melt of PE as a function of pressure points to the increased occurrence of gauche conformers in the high-pressure melt. The CH_2 bending and stretching modes were particularly useful in elucidating chain environment. The PE spectra in these regions differed from those obtained by Takemura et al.[6] This is possibly due to contamination by silicone oil (the pressure-transmitting medium) in their spectra. Since the oil is not miscible with PE, the spectra are simply additive and regions without silicone peaks (e.g., the skeletal optical region) are identical with those obtained in the present study.

Raman spectroscopy should be particularly useful in addressing the question of whether the hexagonal phase is a necessary precursor for the formation of the ECC. A very useful mode exists at low frequency. This is the longitudinal acoustic mode (LAM). The LAM is the accordion-like vibration of an all-trans lamellar structure. The frequency of the LAM is inversely proportional to lamellar thickness. It should be possible to observe the LAM in the region thought to be a mixed-phase region. This type of observation would make possible a determination of the effect of annealing on lamellar structures in this region. In particular, it would be determined if the lamellar thickness increases or the lamellar structure simply disappears on annealing. Work in this direction is being pursued.

Acknowledgment. I am indebted to Dr. William Daniels and Dr. Paul Keyes of the University of Delaware for the loan of the high-pressure cell and invaluable assistance and advice on its use. Particular thanks are due to Dr. Richard G. Priest of the Naval Research Laboratory for helpful and stimulating discussions on this problem and for critically reading the manuscript. I gratefully acknowledge the partial support of Naval Air Systems Command for this research.

References and Notes

(1) Bassett, D. C.; Turner, B. *Nature (London), Phys. Sci.* **1972**, *246*, 146. *Philos. Mag.* **1974**, *29*, 925.
(2) Yasuniwa, M.; Nakafuku, C.; Takemura, T. *Polym. J.* **1973**, *4*, 526.
(3) Bassett, D. C.; Block, S.; Piermarini, G. J. *J. Appl. Phys.* **1974**, *45*, 4146.
(4) Leute, U.; Dollhopf, W. *Colloid Polym. Sci.* **1980**, *258*, 353.
(5) Takemura, T. *Polym. Prepr., Am. Chem. Soc., Div. Polym. Chem.* **1979**, *20*, 270.
(6) Tanaka, H.; Takemura, T. *Polym. J.* **1980**, *12*, 349.
(7) Yasuniwa, M.; Enoshita, R.; Takemura, T. *Jpn. J. Appl. Phys.* **1976**, *15*, 1421.
(8) Yamamoto, T.; Miyaji, H.; Asai, K. *Jpn. J. Appl. Phys.* **1977**, *16*, 1891.
(9) Yasuniwa, M.; Takemura, T. *Polymer* **1974**, *15*, 661.
(10) Schoen, P. E.; Priest, R. G.; Sheridan, J. P.; Schnur, J. M. *J. Chem. Phys.* **1979**, *71*, 317.
(11) Lippert, J. L.; Peticolas, W. L. *Proc. Natl. Acad. Sci. U.S.A.* **1971**, *68*, 1752.
(12) Lippert, J. L.; Peticolas, W. L. *Biochim. Biophys. Acta* **1972**, *282*, 8.
(13) Faiman, R.; Larsson, K. *J. Raman Spectrosc.* **1976**, *4*, 387.
(14) Bulkin, B. J. *Appl. Spectrosc.* **1976**, *30*, 261.
(15) Gaber, B. P.; Peticolas, W. L. *Biochim. Biophys. Acta* **1977**, *465*, 260.
(16) Gaber, B. P.; Yager, P.; Peticolas, W. L. *Biophys. J.* **1978**, *21*, 161.
(17) Bulkin, B. J.; Yellin, N. *J. Phys. Chem.* **1978**, *82*, 821.
(18) Zerbi, G.; Abbate, S., to be published in *Chem. Phys. Lett.*
(19) Snyder, R. G.; Hsu, S. L.; Krimm, S. *Spectrochim. Acta, Part A* **1978**, *34a*, 395.
(20) Snyder, R. G.; Scherer, J. *J. Chem. Phys.* **1979**, *71*, 3221.
(21) Wunder, S. L.; Schoen, P. E., to be published in *J. Appl. Phys.*
(22) Tasumi, M.; Shimanouichi, T.; Miyazawa, T. *J. Mol. Spectrosc.* **1962**, *9*, 261.
(23) Strobl, G. R.; Hagedorn, W. *J. Polym. Sci., Polym. Phys. Ed.* **1978**, *16*, 1181.
(24) Merajver, S. D.; Yorke, E. D.; DeRocco, A. G. *Phys. Rev. A.* **1981**, *23*, 2.
(25) Synder, R. G.; Scherer, J. R.; Gaber, B. P. *Biochim. Biophys. Acta* **1980**, *601*, 47.
(26) Wunder, S. L.; Merajver, S. D. *J. Chem. Phys.* **1981**, *74*, 5341.
(27) Barnes, J. D.; Fanconi, B. M. *J. Phys.* **1972**, *56*, 5190.
(28) Schoen, P. E.; Priest, R. G.; Sheridan, J. P.; Schnur, J. M. *J. Chem. Phys.* **1979**, *71*, 317.
(29) Devaure, J.; Lascombe, J. *Nouv. J. Chim.* **1979**, *3*, 579.